Figure S1. Forest plots of univariate and multivariate Cox analyses. (A) Univariate Cox analyses in TCGA cohort. (B) Multivariate Cox analysis in TCGA cohort. TCGA, The Cancer Genome Atlas.

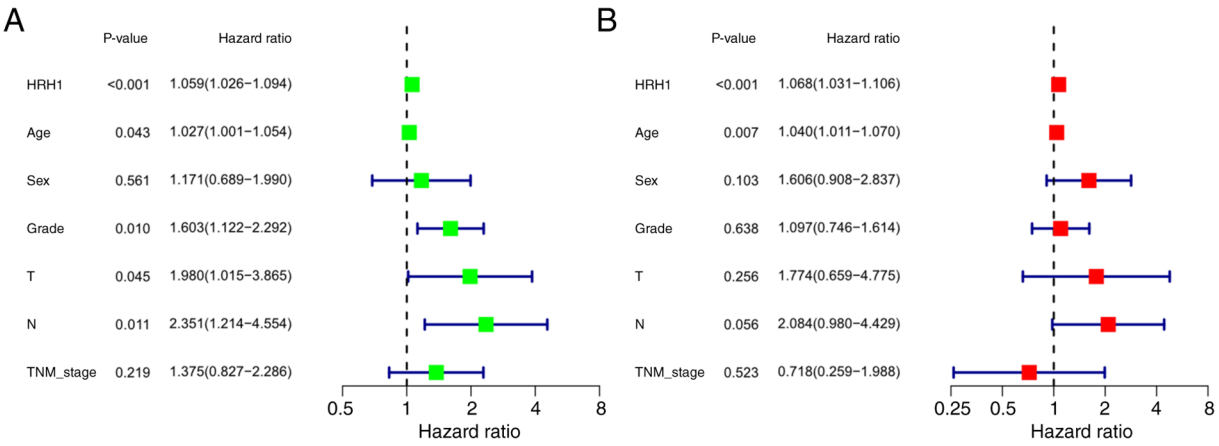

Figure S2. Association between HRH1 expression and resistance to doxorubicin, platin, mitomycin and vincristine.

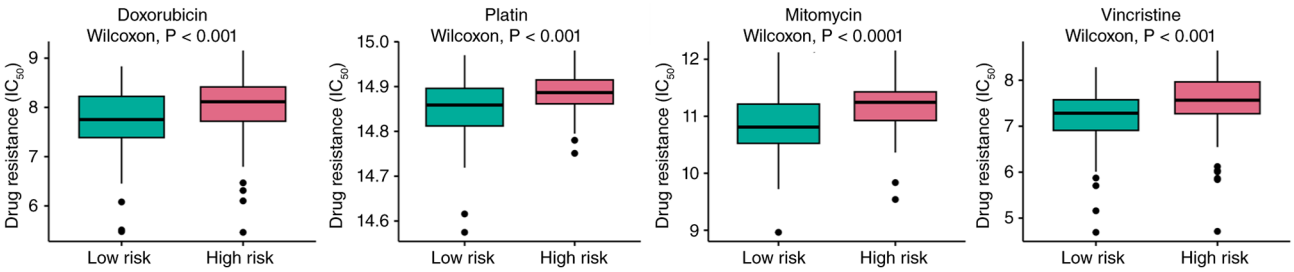

Figure S3. Forest plot and Funnel plot of the MR analysis. (A) The individual SNP final selected for the effect of fexofenadine treatment on pancreatic cancer. (B) Funnel plot used to evaluate potential heterogeneity in the MR analysis. MR, Mendelian randomization.

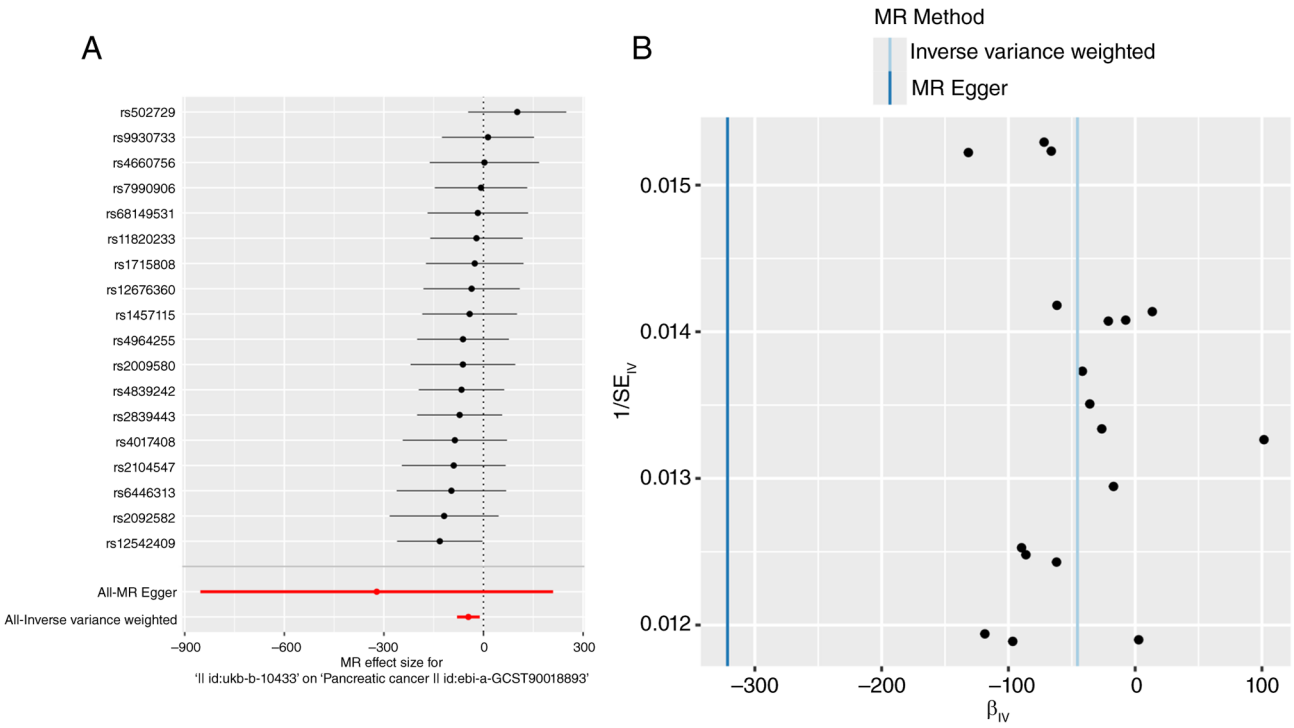

Figure S4. Reciprocal regulation between HRH1 and YAP1 across various human cell lines. (A) In human endothelial cells, knockdown of HRH1 led to downregulation of several YAP1 target genes. Transcriptomic analysis revealed that YAP1 silencing markedly downregulated HRH1 expression across multiple cell lines, including (B) MDA-MB-231, (C) NLF, (D) HepG2 and (E) RCC4. The knockdown groups were compared with the non-targeting control in each cell line. *P<0.05, **P<0.01; ***P<0.001; ****P<0.0001). NC, negative control; KD, knockdown; si, small interfering.

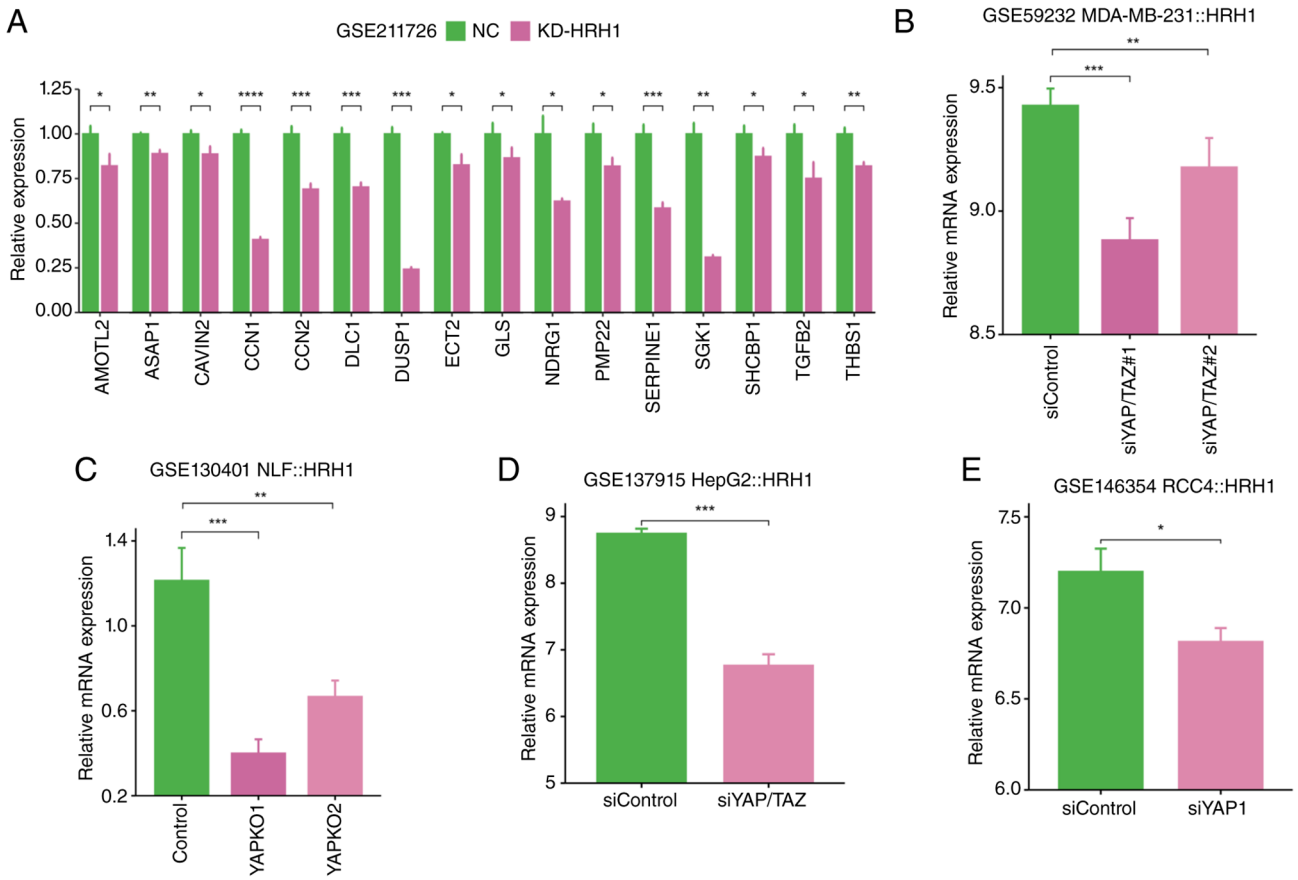

Figure S5. PCA plots before and after batch effect correction. (A) PCA plot before batch effect correction. (B) PCA plot after batch effect correction. PCA, principal component analysis.

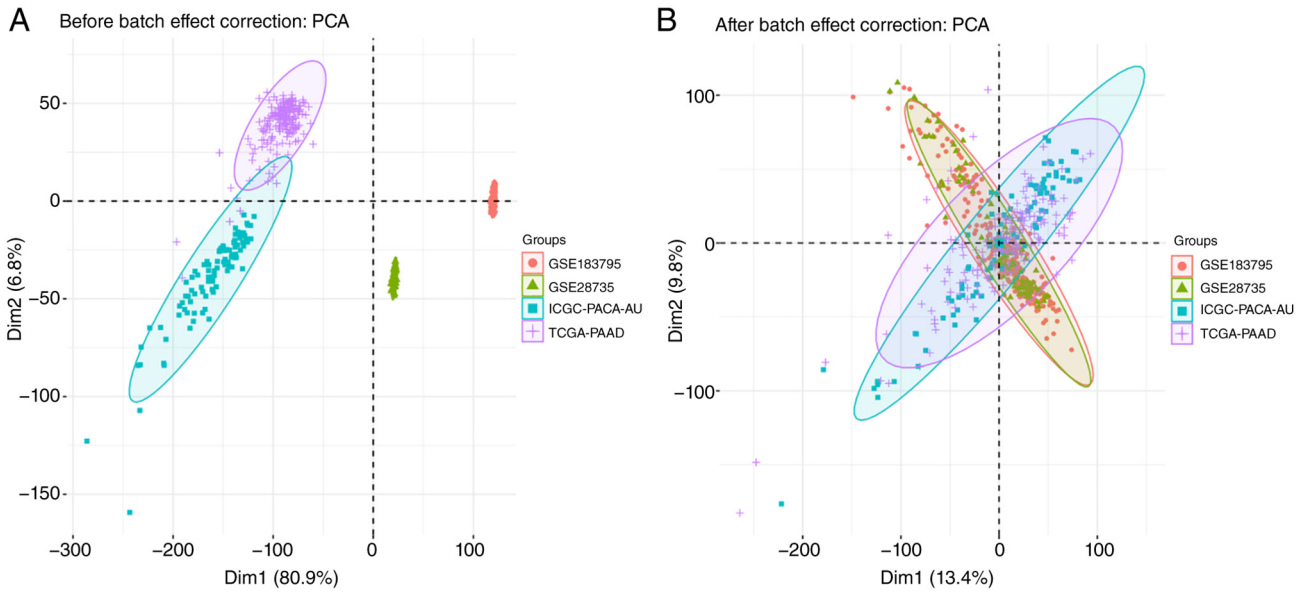

Figure S6. The time-dependent Brier scores for 1-, 2-, 3- and 4-year overall survival prediction in three independent cohorts. (A) TCGA-PAAD cohort. (B) ICGC-PACA-AU cohort. (C) GEO cohort.

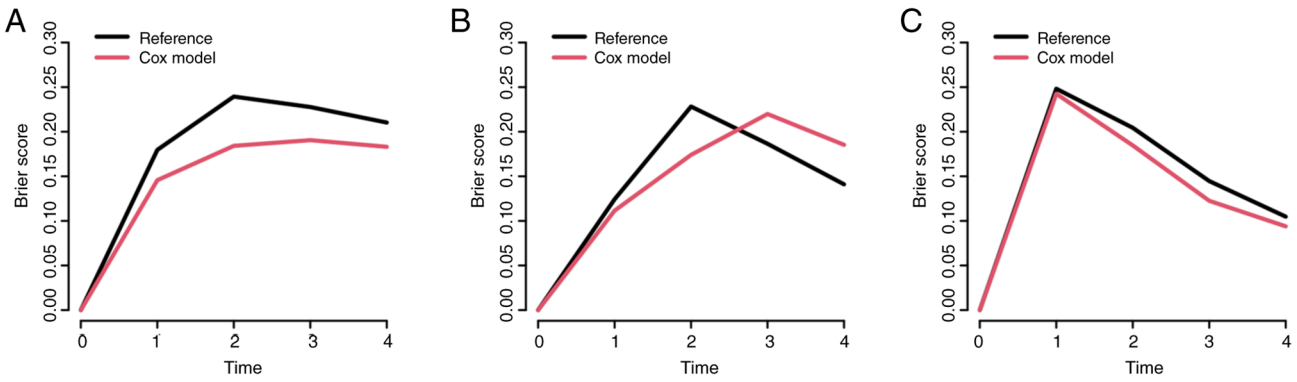

Figure S7. Evaluation of the correlation between risk score and tumor-infiltrating immune cell abundance.